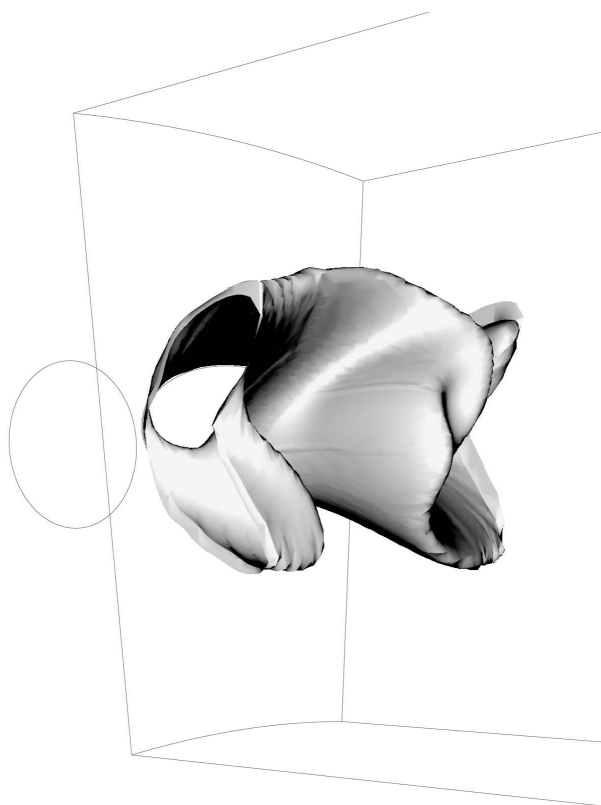




AIAA 2001-2104

**Impact of the Fuel Time Lag
Distribution in Elliptical Premix
Nozzles on Combustion Stability**

Wolfgang Polifke, Jan Kopitz, Ana Serbanovic
Lehrstuhl für Thermodynamik,
Technische Universität München,
D-85747 Garching, Germany



7th AIAA/CEAS Aeroacoustics Conference
May 28–30, 2001/Maastricht, The Netherlands

Impact of the Fuel Time Lag Distribution in Elliptical Premix Nozzles on Combustion Stability

Wolfgang Polifke *

Jan Kopitz †

Ana Serbanovic ‡

*Lehrstuhl für Thermodynamik,
Technische Universität München,
D-85747 Garching, Germany*

The impact of premix nozzle shape on combustion stability in a geometry representative of an annular low-emission combustor is investigated by a combination of numerical and analytical means. For three elliptical premix nozzle geometries with varying eccentricity, the flame shape is computed with computational fluid dynamics using a standard stationary Reynolds-averaged formulation with Reynolds-Stress and turbulent flame speed closure models. From the CFD solution, the time lags for convective transport from the fuel injector to the flame front are determined through Lagrangian particle tracking. Interpreting the histograms of particle arrival times as the unit impulse response of fuel consumption to a perturbation of fuel injection, the corresponding fuel transport frequency response $F(\omega)$ is computed and used to achieve closure for a linear acoustic model of the behavior of a compact premix flame. Using this model for the flame dynamics in a network model of linear acoustics in annular geometries, the impact of nozzle shape and fuel transport time lag distribution on the thermo-acoustic stability of a premixed combustor is explored. For the configurations investigated, the elliptical premix nozzles produce wider time lag distributions with smaller mean values than the circular base configuration and are less prone to combustion instabilities.

Introduction

Combustion instabilities in premixed systems are a very active field of research of great applied significance for stationary as well as airborne gas turbines and other combustion devices. Fundamental investigations of the mechanisms leading to instabilities, the thermo-acoustic characteristics of enclosed premixed flames as well as passive or active means of instability control are being investigated by experimental, numerical and analytical means.

Fluctuations of the fuel equivalence ratio have been identified as one possible cause for combustion instabilities.¹⁻⁵ For this mechanism, the time required for fuel particles to travel from the fuel injector to the flame front – simply referred to as the *fuel time lag* in this paper – is the dominant stability parameter. Detun-

ing the time lag relative to the combustor's acoustic eigenmodes is one viable means of passive control.^{2,5} However, it is practically impossible to detune the fuel time lag with respect to all eigenmodes of a combustor. It follows that a change in mean fuel time lag, e.g. by shifting the location of fuel injection, may stabilize one mode while rendering another mode unstable.

Sattelmayer⁶ has emphasized that not only the mean time lag controls combustion stability, but also the distribution of the time lag resulting from convective dispersion of injected fuel. In general, widening the time lag distribution weakens the feedback loop between combustor acoustics, fuel concentration and heat release rate fluctuations and should reduce the propensity towards thermo-acoustic instability. Staggering the fuel injection within one burner² or using different types of burners in one combustor⁵ therefore appears to be a rather robust method of control.

Another method of passive control that has been investigated is the use of non-circular fuel nozzles or burners^{5,7} with the rationale that breaking the az-

*Professor, polifke@td.mw.tum.de

†Doctoral Student, kopitz@td.mw.tum.de

‡IAESTE Exchange Student, serbanov@td.mw.tum.de

Copyright © 2001 by the American Institute of Aeronautics and Astronautics, Inc. All rights reserved.

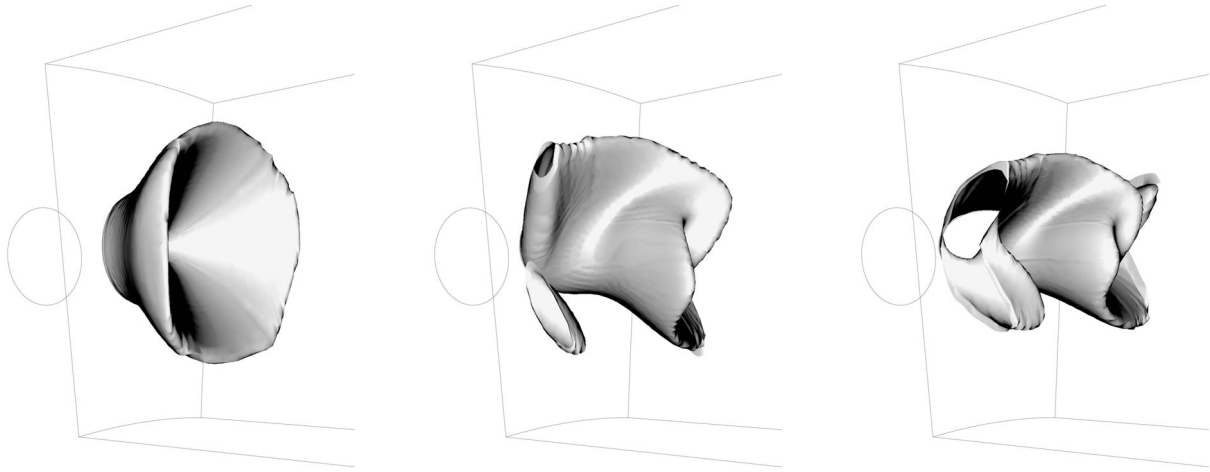


Fig. 1 Flame shape for different nozzle geometries. **Left:** base configuration ($a:b = 1.0$). **Middle:** elliptical nozzle outlet with $a:b = 1.5$. **Right:** $a:b = 2.0$.

imutal symmetry of the swirling flow exiting a nozzle suppresses the growth of large scale coherent vortical structures, which could otherwise strongly modulate the rate of heat release in a periodic fashion. The importance of large scale vortical coherent structures for combustion has been emphasized in an extensive review by Coats.⁸ Coherent structures modulate the mixing of fuel, oxidizer and combustion products and thereby can influence the rate of heat release as well as formation of pollutants like NO_x or soot. In practical combustion devices, coherent structures may form principally in two ways: 1) fluctuation of the bulk velocity of a separating flow injects vorticity into the flow at a non-uniform rate. The injected vorticity agglomerates into a coherent vortex due to self-induction. 2) inherent fluid-dynamic instabilities characteristic of the base flow grow into large-amplitude vortical structures. In the context of combustion instabilities, coherent structures may be interpreted as a root cause of an instability in the latter case, while they may act as a strong mechanism of amplification in the first case.

From the point of view of a burner or combustor designer, swirling flows are of particular importance. Unfortunately, studies of coherent structures in reacting swirling flows are scarce. In a strongly swirling flow with vortex breakdown, as one might find it in a modern low-emission premix burner, a precessing vortex core and asymmetric axial velocity distributions were observed.^{9,10} Coats comments that a helical secondary vortex is associated with the precessing vortex core, possibly resulting from the excitation of a helical instability mode of the flow. This aspect has been further explored by Paschereit et al., who investigated fluid dynamic instabilities in a swirl-stabilized experimental premix burner by experimental and analytical means.^{11,12} Linear stability analysis using a spectral collocation method was applied to measured profiles of axial and tangential velocity at the

burner dump plane. The computations confirmed observations made in non-reacting flow, i.e. the flow is susceptible to both helical and axisymmetric disturbances. The most strongly amplified instability mode is the counter-rotating helical one. In an atmospheric combustion test rig, thermo-acoustic combustion instabilities were observed with symmetry and Strouhal numbers corresponding to the non-reacting case. The helical mode, while clearly the dominant fluid-dynamic instability, produced lower combustion noise than the axisymmetric mode. This is explained by observing that non-axisymmetric acoustic modes are evanescent at the comparatively low frequency of the helical instability.

In non-circular jets, the growth of coherent structures is often strongly suppressed due to vortex deformation and self induction processes in the non-axisymmetric flow field, which leads to early breakup of coherent structures, increased entrainment and enhanced fine-scale mixing.⁷ In several applications including combustion, the use of non-circular nozzle geometries has been found to provide a powerful yet inexpensive means of (passive) instability control.⁷ A first successful application of this technique to a swirl-stabilized premix burner has already been reported,⁵ however, the mechanism by which the “asymmetrical burner outlet” reduces combustion instabilities has not yet been identified precisely.

The present paper contributes to the development of a consolidated view on the two control methods discussed above, i.e. modulating the time-lag and employing non-circular nozzles. It is argued that differences in flame shape between a circular and non-circular burner will in general also result in a different time lag distribution and thereby alter combustion stability characteristics. A combined analytical and numerical approach is developed: CFD simulations of the reacting flow field in circular and non-circular versions

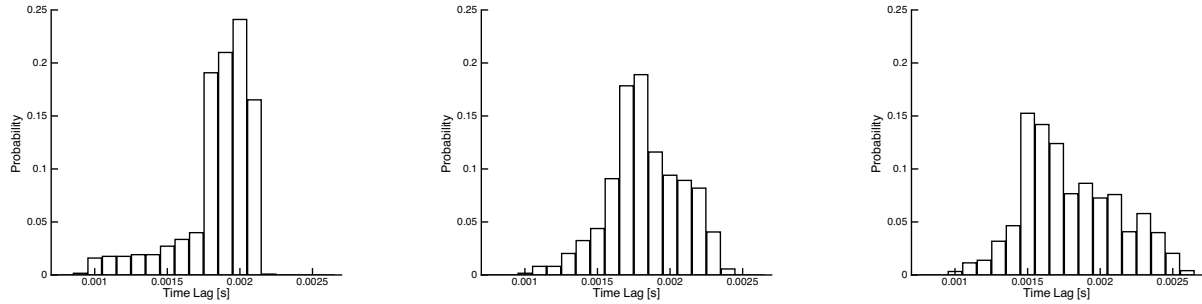


Fig. 2 Unit impulse response of the fuel injection for a (from left to right) circular, elliptic with $a:b = 1.5$ and elliptic with $a:b = 2.0$ combustor inlet.

of a burner of generic design are performed in order to determine the respective time lag distributions by Lagrangian particle tracking. The distributions obtained in this manner can be used in linear stability analysis, using a network model of the combustor.^{1,6,13–17} For this purpose, the time lag distribution is interpreted as the unit impulse response of convective fuel transport, i.e. the response of fuel consumption at the flame to a unit impulse perturbation of fuel injection. In principle, this approach allows a quantitative prediction of the impact of fuel time lag distributions of arbitrary shape on combustion stability. In the light of the results obtained, the explanations offered until now for the impact of non-circular nozzle geometries on combustion stability, are critically appraised.

CFD Model and Results

Model Details

The burner geometry investigated is of generic design: from a "mixing tube" with varying cross-sectional shape, a swirling flow enters a cavity, which represents a segment of an annular combustor of a medium-size stationary gas turbine. The radius of the combustor annulus is of the order of 1 m, its axial extent is one half of this value. It is implied that a swirler/ fuel injector is located just upstream of the computational domain; experimentally measured profiles of axial and circumferential velocity components as well as estimates for turbulent intensity and length scale are set accordingly at the inlet plane. In the reacting flow simulation, the fuel-air mixing process is not resolved in detail, as it is assumed that the fuel-air mixture is well homogenized before it reaches the flame front.

The mixing tube is of circular cross section at the upstream end, while it is elliptical – with varying aspect ratio $a:b$ of major to minor axis – at the downstream side. In studies of flow control with non-circular jets, aspect ratios of typically 5:1 and as large as 20:1 have been employed.⁷ However, in the present case the nozzle flow possesses significant swirl, and it was feared that with high aspect ratios flow separation and local recirculation in the apices of the elliptical

nozzle might occur. Therefore the maximum aspect ratio $a:b$ investigated in this study equals 2; CFD results indicate that the swirling flow is well able to follow the shape of such a nozzle. The area of the elliptic nozzle outlets was the same as its circular counterpart so that no change in the mean flow velocity is induced by the distortion of the nozzle shape.

In order to numerically calculate the reacting flow, the domain has been discretized on a block structured hexagonal grid for use with the commercial CFD package FLUENT. The grid has been partly refined for the purpose of accurately resolving the swirling flow. This leads to grid cells the size of less than 0.5mm and a total number of more than 700000 cells, thus the grid has not been depicted here.

It should also be mentioned that the simulation was performed incompressibly in the sense, that the density is computed from the equation of state using the temperature – computed from the combustion progress variable c – and the mean operating pressure. The turbulent flow and reaction progress are computed with a standard Reynolds-Stress turbulence model (RSM) and the TFC combustion model.^{18,19} The TFC model uses a correlation for the turbulent flame speed, which involves the laminar flame speed, turbulent intensity and length scale, a critical stretch rate and various material properties. Laminar flame speeds are determined from computations of one-dimensional laminar premix flames with detailed chemistry for methane-air combustion with an oxidizer to fuel ratio $\phi = 0.45$. The critical rate of strain g_{cr} is difficult to determine for high pressures,²⁰ therefore it has been set to a very high value $g_{cr} \rightarrow \infty$, effectively neglecting the effects of turbulent stretch on flame propagation. Given that the present study investigates a generic situation, this approximation is justifiable. Turbulence properties and material parameters required for the correlation are taken (locally) from the CFD simulation.

The subject of the present work is combustion instability, it might appear inappropriate that an incompressible, Reynolds-averaged, steady state approach was chosen. However, the goal of the CFD studies was to determine the flame shape and the corresponding

distribution of fuel transport time lags (see below) resulting from the different nozzle geometries. The time lag distribution is then used in subsequent thermoacoustic stability analysis (see below).

Influence of Nozzle Geometry on Flame Shape and Time Delay Distribution

Figure 1 shows calculated flame shapes (iso-surfaces $c = 0.8$ of the calculated progress variable) for circular respectively elliptical combustor inlets with different aspect ratios. It impressively demonstrates the strong influence of the premix nozzle shape on the spatial distribution of heat release. While the flame surface in the combustor with the conventional circular inlet is a nearly symmetrical cone, with increasing aspect ratio the shape appears more and more three-dimensional and convoluted. One should expect that correspondingly the distribution of the time lag for convective transport from the fuel injection, i.e. in this case the inlet of the computational domain, to the flame front should become wider with increasing aspect ratio. Ideally, the distribution is represented by a δ -peak at the beginning of the mixing tube and widens as the fuel is transported convectively downstream.

In Figure 2, the fuel transport time lag distributions for the three cases with aspect ratios $a:b = 1, 1.5$ and 2 are presented as histograms. From the stationary velocity fields, the time lag distributions are determined through Lagrangian particle tracking. To this purpose, a cloud of massless particles, distributed evenly across the inlet area (upstream side of the premix nozzle) at time $\tau = 0$, is convected by the flow field until all particles have reached the flame front. The arrival times are recorded to construct histograms as shown in Figure 2. In order to achieve good statistics, 1200 particles are released. As expected, with increasing aspect ratio $a:b$ of the ellipses, the time lag distribution gets wider and its peak lower.

Figure 3 depicts the product formation rate (reaction rate) averaged over combustor cross-sectional area vs. distance from the combustor dump plane. Clearly, the flame corresponding to the circular inlet is more compact. Figure 3 also shows that the heat release is concentrated in a region, which is much shorter than acoustic wavelengths up to frequencies of 1 kHz, say, i.e. for all three geometries investigated the flame may be approximated as an *acoustically compact* flame sheet (see the next Section).

$a:b$	μ [ms]	σ [ms]	Stand Off [mm]	f [Hz]	Cycle Incr. [%]
1.0	1.83	0.243	58	877	1.69
1.5	1.82	0.244	63	883	-4.66
2.0	1.78	0.316	63	880	-12.42

Table 1 Results for the time lag distribution, flame stand off and first eigenmode

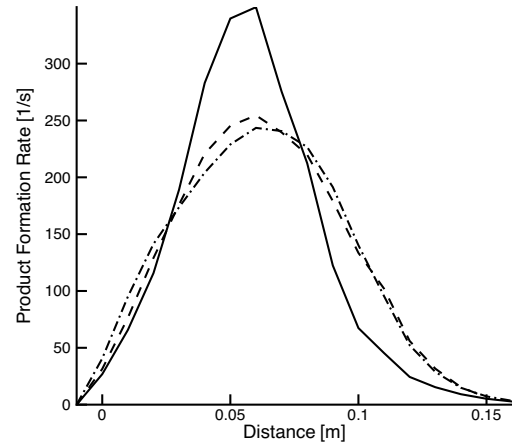


Fig. 3 Distribution of the product formation rate (reaction rate). solid line: $a:b = 1.0$; dashed line: $a:b=1.5$; dash-dotted line: $a:b = 2.0$.

Table 1 gives an overview of the CFD results in terms of mean value μ and standard deviation σ of the time lag distributions as well as the flame stand-off l_F . The latter is defined as the center of mass of the area under the curves in Fig. 3 and is one of the input parameters to the acoustic network model of the combustor discussed in the next Section.

Network Model of a Premixed Combustor

Linear Acoustics in an Annular Combustor

A simple yet quantitative network model of linear acoustics in a premixed combustor is now constructed. The combustor corresponds to the generic design of an annular combustor investigated with CFD in the previous Section, see Fig. 4. A very similar configuration has been used by Polifke et al.¹⁶ in an investigation of the interference of acoustic and entropy waves in a premixed combustor with a choked exit and by Sattelmayer⁶ in a study of the influence of convective wave dispersion on combustion stability. More details on the model formulation and additional discussion of the stability of plane and higher order eigenmodes in this annular combustor as well as the response to a fluid-dynamic excitation mechanism have been published by Polifke et al.¹⁷

From a plenum, air enters a swirler and fuel injection section "1", passes through a mixing section of length L_τ until it encounters at "2" an expansion in cross sectional area with the area ratio $\alpha \equiv A_2/A_3$. The flame front is located between "4" and "5", a short distance from the dump plane. At the combustor exit "6", a compact choked nozzle is located.

Propagation of acoustic waves through this system can be modeled with the following set of equations:

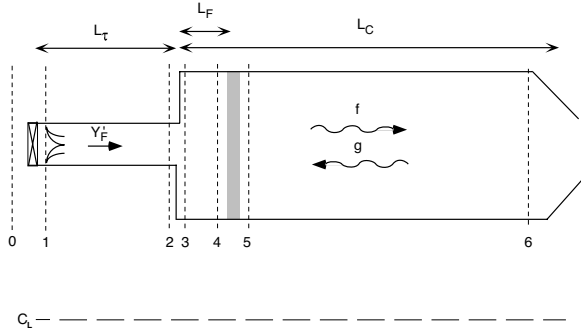


Fig. 4 Quasi-2D model of a premixed annular combustor. "0" - upstream plenum, "1" location of fuel injection, "1"- "2" fuel/air mixing section, "2"- "3" jump in cross-sectional area, "3"- "4" cold section of combustor (*flame stand-off distance*), "4"- "5" flame sheet, "5"- "6" hot section of the combustor, "6" exit nozzle. The acoustic disturbances traveling in the down- and upstream direction are indicated as f and g ("Riemann Invariants").

Upstream boundary ("1")

The difference in mean pressure p between the burner plenum "0" and the location of fuel injection "1" can be described by

$$p_1 - p_0 = -\frac{\zeta}{2}\rho u_1^2,$$

with a pressure loss coefficient ζ . Linearizing this relation and assuming that in the burner plenum acoustic fluctuations of the pressure are absent, $p'_0 = 0$, an upstream boundary condition is obtained:

$$\left. \frac{p'}{\rho c} \right|_1 = -\zeta M_1 u'_1. \quad (1)$$

Primed quantities " ' " denote acoustic variables, i.e. small deviations from the respective mean values.

Area Change ("2" - "3")

Conservation of mass and momentum across the change in cross-sectional area at the burner dump plane with area ratio $\alpha = A_2/A_3$ yields after linearization:

$$\left. \frac{p'}{\rho c} \right|_3 = \left. \frac{p'}{\rho c} \right|_2 - \zeta_A M_3 u'_3 \quad (2)$$

$$u'_3 = \alpha u'_2 \quad (3)$$

where a Borda-type pressure loss coefficient $\zeta_A \equiv (1 - 1/\alpha)^2$ has been introduced.

Compact Premix Flame ("4" - "5")

The zone of heat release in the combustor is modeled as a *flame sheet*, i.e. as a discontinuity of negligible thickness where per unit area heat is added at a certain rate \dot{Q} [W/m²]. Linearizing the Rankine-Hugoniot relations, which express conservation of mass, momentum and energy across the discontinuity, the following

relations coupling fluctuations of velocity and pressure on both sides of the flame sheet are derived:

$$u'_5 = u'_4 + u_4 \Theta \left(\frac{\dot{Q}'}{\dot{Q}} - \frac{p'_4}{p_4} \right), \quad (4)$$

$$\xi \left. \frac{p'}{\rho c} \right|_5 = \left. \frac{p'}{\rho c} \right|_4 - u_4 M_4 \Theta \left(\frac{\dot{Q}'}{\dot{Q}} + \frac{u'_4}{u_4} \right), \quad (5)$$

with a temperature raise coefficient $\Theta \equiv T_5/T_4 - 1$. Density ρ and speed of sound c change across the flame sheet, therefore it is necessary to introduce the ratio of specific impedances $\xi \equiv \rho_4 c_4 / \rho_5 c_5$. With the notation chosen in (5), it is evident that the pressure drop across the flame sheet is of first order in Mach number, corrections to (5) are second order in Mach number. One can also show that the contribution of pressure fluctuations to (4) is of first order in Mach number.

The coupling relations (4) and (5) are not yet closed as they involve the fluctuations \dot{Q}' of the heat release rate, which must be expressed in terms of pressure or velocity fluctuations. The closure assumptions used in the present analysis are based on time-lagged fuel equivalence ratio modulations, linking fluctuations of velocity at the fuel injector at an earlier time $t - \tau$ to variations of the heat release rate $\dot{Q}'(T)$. This will be discussed in detail in the next Section, where the flame transfer matrix is derived.

Exit condition ("6")

The boundary conditions for the choked combustor exit are taken from work of Marble and Candel²¹

$$u'_6 = M_6 \frac{\gamma - 1}{2} \left. \frac{p'}{\rho c} \right|_6, \quad (6)$$

where $\gamma \equiv c_p/c_v$ denotes the ratio of specific heats.

Wave propagation ("1" - "2", "3" - "4", "5" - "6")

With harmonic acoustic waves traveling back and forth in an annular duct of length l , the following relation holds between the fluctuations of pressure and velocity at the downstream ("d") and upstream ("u") ends:

$$\begin{pmatrix} \left. \frac{p'}{\rho c} \right|_d \\ u'_d \end{pmatrix} = \begin{pmatrix} \cos(k_x l) & i \sin(k_x l) \\ i \sin(k_x l) & \cos(k_x l) \end{pmatrix} \begin{pmatrix} \left. \frac{p'}{\rho c} \right|_u \\ u'_u \end{pmatrix}, \quad (7)$$

The axial wave number is determined from

$$k_x^2 = \left(\frac{\omega}{c} \right)^2 - k_\perp^2, \quad (8)$$

where the perpendicular wave number k_\perp is non-zero only for higher order acoustic modes. Corrections due to the mean flow, which are of second order in Mach number for the pressure and velocity fluctuations, are neglected.

For numerical solution of this set of equations, the model is conveniently formulated in terms of the *Riemann invariants* f and g instead of the fluctuations of

pressure p' and velocity u' . The Riemann invariants f, g – sometimes also referred to as p'^+ and p'^- – are fundamental solutions of the wave equation and may be interpreted as acoustic waves traveling in the positive (downstream) or negative (upstream) direction, respectively.¹ The following relations hold between fluctuations of velocity u' and pressure p' and the Riemann invariants

$$\frac{p'}{\rho c} = f + g, \quad (9)$$

$$u' = \chi(f - g), \quad (10)$$

where $\chi = \sqrt{1 - (k_{\perp}/k)^2}$ for higher order acoustic modes. More details on the formulation of the above system of equations with the Riemann invariants are given in Polifke et al.¹⁷

Entropy waves are not considered in the present study, although a complete thermo-acoustic analysis of a combustor with choked exit should include entropy waves.¹⁷ However, it is felt that for the present purposes the inclusion of entropy waves would only result in extra complexity without providing the benefit of additional insight.

Closure of the flame sheet model.

The linearized Rankine-Hugoniot relations across the flame sheet (4) and (5) describe how fluctuations of the heat release rate \dot{Q}' couple with the combustor's acoustic modes. In order to obtain a closed homogeneous system of equations characterizing the thermo-acoustic stability of the combustor, it is necessary to express in turn the heat release fluctuations in terms of acoustic variables u' and p' . In this work, it is assumed that inhomogeneities in fuel mass fraction Y'_F caused by fluctuations of pressure p'_1 and velocity u'_1 at the fuel injector control the momentary heat release rate \dot{Q}' . Ignoring for the moment convective dispersion of fuel inhomogeneities, the coupling between fluctuations in velocity and pressure at the fuel injector and heat release rate may be described by the following expression:

$$\frac{\dot{Q}'(t)}{\dot{Q}} = -\frac{1}{2} \frac{p'_1(t - \tau)}{\Delta p} - \frac{u'_1(t - \tau)}{u(x_1)}. \quad (11)$$

Here the unprimed quantities denote mean values, and $\Delta p = p_{\text{Nozzle}} - p_1$ is the mean pressure drop across the fuel injector. A *time lag* τ must be introduced here because the heat release rate will not respond instantaneously to fluctuations of fuel mass fraction Y'_F , but only after the inhomogeneities have been convected from the fuel injector to the region of heat release.

The first term on the r.h.s of (11) is due to variations in fuel mass flow rate \dot{m}'_F caused by pressure fluctuations. A minus sign appears in front of the pressure term in (11), because a momentary increase of pressure in the premixing duct reduces the fuel mass flow

rate,

$$\frac{\dot{m}'_F}{\dot{m}_F} = -\frac{1}{2} \frac{p'_2}{\Delta p}, \quad (12)$$

In premixed low-emission combustion systems, the pressure drop Δp is often quite large in order to provide sufficient momentum for rapid mixing of fuel and combustion air. In this case, the fuel injection system is "stiff", i.e. the fuel injection rate does not respond significantly to acoustic perturbations. Therefore, the first term on the r.h.s. of (11) is neglected in the present analysis.

Nevertheless, acoustic perturbations of the *air* flow u'_1 at the fuel injector will cause fluctuations of fuel mass fraction Y'_F and subsequently variations in heat release rate \dot{Q}' . This phenomenon is accounted for by the second term in (11). The minus sign is appropriate, because a momentary increase in air flow past the fuel injector will lower the fuel concentration and lead to a corresponding reduction of the heat release rate.

As already mentioned, this reduction does not occur instantaneously, but after a time lag τ . The mean time lag can be estimated as the residence time in the fuel-air mixing section and the "cold" section of the combustor upstream of the flame, i.e.

$$\tau \approx \frac{L_{\tau}}{u_1} + \frac{L_F}{u_3}, \quad (13)$$

where u_1 and u_3 are mean velocities based on the average volume flux and the respective cross-sectional areas of mixing tubes and combustion chamber. For harmonic perturbations $\sim \exp(i\omega t)$ with angular frequency ω , this leads to the following closure relation:

$$\frac{\dot{Q}'}{\dot{Q}} = e^{-i\omega\tau} \frac{u'_1}{u_1}. \quad (14)$$

However, Sattelmayer⁶ has demonstrated that this idealized formulation, which ignores convective dispersion of fuel inhomogeneities, is appropriate for the analysis of real combustion systems only at sufficiently low frequencies. Boundary layers, recirculation zones, etc., result in non-uniform distributions of velocity in the mixing section and the combustor, resulting in significant "smearing out" of fuel (or entropy) inhomogeneities. Turbulent fluctuations contribute also to the dispersion of convectively transported quantities. Furthermore, a flame sheet of axial extent l , which may be considered acoustically compact, $l \ll \lambda = c/f$ at a certain frequency f may very well be not compact for convective waves due to the much shorter wavelength u/f of convective waves, resulting also in a more smeared out response of the heat release rate to perturbations of the fuel concentration generated at the injector.

As a consequence, a distribution of delay times must be considered instead of one single delay time τ (representing the limiting case of a δ -distribution) when

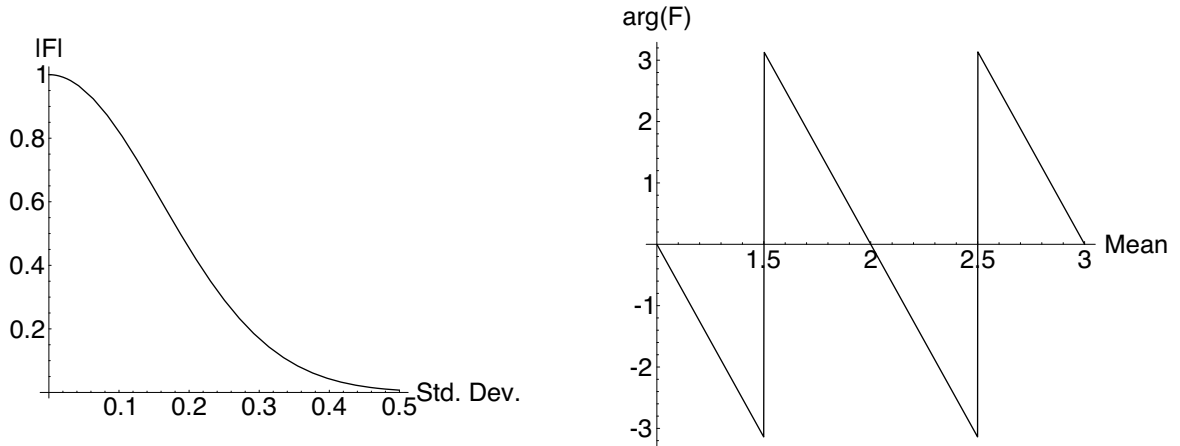


Fig. 5 Fuel transport frequency response for Gaussian time delay distributions (unit impulse response \vec{h}) with mean μ and standard deviation σ . **Left:** absolute value $|F|$ vs. normalized standard deviation σf and arbitrary mean value. **Right:** phase $\arg(F)$ vs. normalized mean value μf and arbitrary standard deviation.

determining the closure relations for the heat release fluctuations. To this purpose, Sattelmayer⁶ has assumed a certain idealized shape for the distribution of delay times, characterized by a mean time lag $\bar{\tau}$, a width $\Delta\tau$ and a "slope parameter" ΔC . The Laplace transform of the presumed distribution of delay times then yields in analytical form the frequency response between equivalence ratio modulations at the fuel injector and heat release rate required for closure.

Unfortunately, the distributions of delay times found with CFD (see Fig. 2) do not much resemble the time lag pdf presumed by Sattelmayer.⁶ Clearly, a more general formulation is called for, which is able to handle arbitrary distributions of the time delay. The required mathematical tools have been developed in communications engineering, in particular *system identification*.^{22,23} These methods have been applied to thermo-acoustic problems by Polifke et al. in an effort to reconstruct the transfer matrix of a heat-source with time lag from instationary CFD computations.^{24,25} Using this formalism, the response \vec{h} of the fuel mass fraction at the flame front to a "unit impulse" perturbation of the fuel mass fraction at the injector is the fundamental quantity to describe the propagation and dispersion of the convective "fuel wave". A little consideration shows that indeed the time lag histograms obtained from particle tracking in the CFD model may be directly interpreted as the unit impulse responses \vec{h} . The frequency response $F(\omega)$ of convective fuel transport is then computed as the z -transform of \vec{h} with argument $z = i\omega\Delta t$:

$$F(\omega) = \sum_0^{\infty} h_k e^{-i\omega\Delta tk}. \quad (15)$$

Here Δt is the width of the bins in the time lag his-

togram, h_k the value of the k th bin. Of course, in practice the summation extends only over bins with non-zero entries. The frequency response $F(\omega)$ can be determined easily numerically for arbitrary time lag distributions / unit impulse responses \vec{h} and frequencies ω . Closure for the heat release rate fluctuations is then provided by the following expression:

$$\frac{\dot{Q}'}{\dot{Q}} = e^{-i\omega t} F(\omega) \frac{u_1'}{u_1}. \quad (16)$$

Thermo-Acoustic Stability Analysis

Results obtained with Gaussian Time Delay Distribution

Before exploring the effects of premix nozzle geometry on time delay distribution and combustion stability, a few basic results and general trends concerning time delay distributions, fuel transport frequency response and system stability are presented and discussed. For this purpose, we assume without essential loss of generality a Gaussian distribution of time delays with mean μ and standard deviation σ . The absolute value and phase of the fuel transport frequency response $F(\omega)$ corresponding to Gaussian distributions with varying mean and width are shown in Fig. 5. The left plot shows the absolute value $|F(\omega)|$ as a function of the standard deviation σ normalized with the period $2\pi/\omega = 1/f$ of the oscillation. The magnitude of the frequency response (the "gain") decreases with increasing spread of the time lag and indeed vanishes once the standard deviation is equal to or larger than approximately one half of the period. Note that $|F(\omega)|$ does not depend on the mean value μ . Conversely, the phase $\arg(F)$ (right plot in Fig. 5) does not depend on the standard deviation, while it decreases by 2π , when the mean value increases by one period of the oscil-

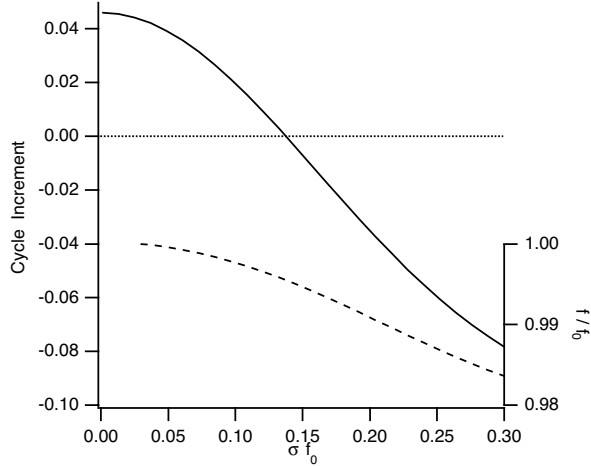


Fig. 6 Cycle increment (—, left axis) and frequency (---, right axis) of the dominant instability mode vs. standard deviation σ of the fuel time lag distribution. Assumed was a Gaussian time lag distribution with a mean value $\mu = 1.87$ ms (or $\mu f_0 = 1.65$ corresponding to the circular premix nozzle geometry).

lation. This expresses the well-known fact that with increasing time lag, heat release fluctuations go in and out of phase with respect to combustor acoustics.^{2,3,17}

How do the changes in fuel transport frequency response with mean and standard deviation of the fuel time lag affect combustion stability? Solving the characteristic equation of the homogeneous system of equations (1) - (7) representing linear acoustic wave propagation and transmission for the combustor shown in Fig. 4, Polifke et al. identified a dominant azimuthally symmetric instability mode with a frequency f_0 near 880 Hz.¹⁷ The mode was very strongly unstable; a cycle increment¹ of 0.4 was found. This was judged to be unrealistically large and attributed to the neglect of loss mechanisms, e.g. Borda-losses at the area expansion, in the model formulation used.¹⁷ With the present model formulation, which includes Borda-losses and convective dispersion of injected fuel, more realistic values of the cycle increment below 0.1 are obtained. Cycle increment and frequency of the dominant instability mode computed with Gaussian time lag distributions are shown in Figs. 6 and 7 for various values of standard deviation σ and mean value μ . In these and the following plots, the frequency f_0 of the dominant mode computed without convective dispersion of fuel ($\sigma \rightarrow 0$) is used for non-dimensionalization. The decreasing gain of the fuel transport $|F(\omega)|$ with increasing width of the time lag distribution significantly reduces the cycle increment

¹The cycle increment is defined as $\exp\{-\Im(\omega)/2\pi\Re(\omega)\} - 1$ and equals the fraction by which the amplitude of an infinitesimal perturbation grows during one cycle. Negative cycle increments indicate stability.

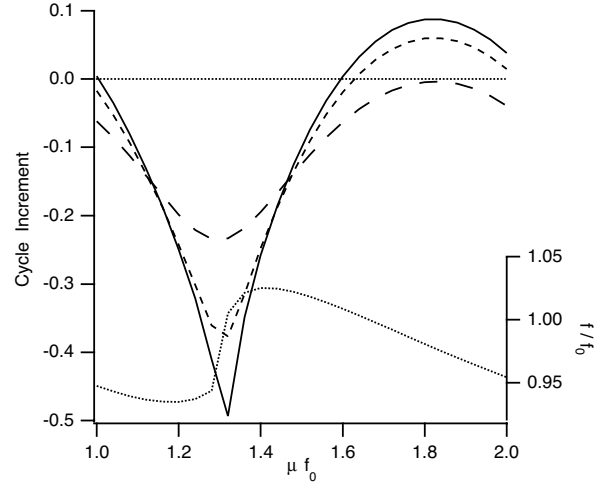


Fig. 7 Cycle increment and frequency of the dominant instability mode vs. mean value μ of the fuel time lag distribution. Assumed was a Gaussian time lag distribution with non-dimensionalized standard deviations $\sigma f_0 = 0$ (—), 0.1 (---) and 0.2 (- · -). For the frequency (\cdots , right axis), only the case with vanishing standard deviation is shown. The CFD results presented above yielded $\sigma f_0 = 0.22 - 0.28$ for the circular and the strongly elliptical case, respectively.

and indeed stabilizes the mode for standard deviations corresponding to 15 % of the oscillation period or larger. The frequency f of the mode depends only weakly on the standard deviation.

A strong sensitivity of the eigenmode's frequency and stability to changes in the mean fuel transport time is shown in Fig. 7. If the time lag distribution is very narrow ($\sigma \rightarrow 0$), the cycle increment increases from -0.5 to 0.1 while the mean value μ varies by one half of the oscillation period. The frequency changes by more than 10 %. With increasing standard deviation σ , this sensitivity is less pronounced and indeed vanishes for $\sigma > 0.5$ (not shown).

The results of stability analyses making use of Gaussian distributions of the fuel transport time lag confirm the conclusions of earlier studies:^{2,3,6,16} combustion stability is very sensitive to changes in the mean value of the fuel transport time lag, while an increase of the width of the time lag tends to stabilize unstable modes.

Impact of Nozzle Geometry on Combustion Stability

It was shown above that for the generic combustor design investigated, changing the premix nozzle geometry from circular to elliptic resulted in a distorted flame shape and a wider time lag distribution with smaller mean value. The fuel transport frequency response for the three geometries investigated is shown in Fig. 8. It is seen that the gain $|F(\omega)|$ is significantly reduced for the elliptical exit geometries, in particular so for higher frequencies, while the phase changes more

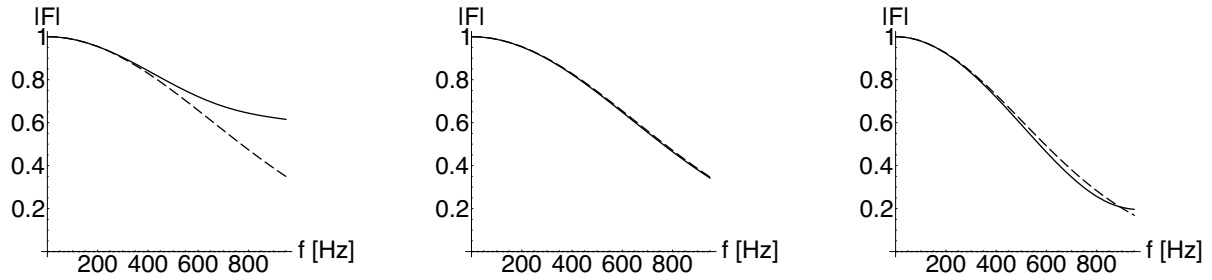


Fig. 8 Absolute value of the fuel transport frequency response function $|F|$ computed from particle arrival time histograms obtained with premix nozzle aspect ratios $a:b = 1$ (left), 1.5 (middle) and 2.0 (right). Shown is also (---) the response function $|F|$ computed from Gaussian time lag distributions with identical mean μ and standard deviation σ , see Table 1.

rapidly.

Near the dominant eigenfrequency $f_0 \approx 880$ Hz of the combustion system, the gain is approximately 0.6 for the circular geometry, while it is around 0.4 and 0.2 for the elliptical premix nozzle outlets with $a:b = 1.5$ and 2.0, respectively. This reduction in gain stabilizes the combustor for the network model investigated: while the circular geometry was computed to be unstable with a cycle increment of 1.7 %, the two elliptic configurations are stable with cycle increments of -4.7 % and -12.4 %, respectively.

Returning to Table 1, we notice that the standard deviation of the fuel time lag increases from 0.24 ms ($\sigma f_0 \approx 0.21$) for the circular geometry to 0.32 ms ($\sigma f_0 \approx 0.28$) for the strongly elliptical one with aspect ratio $a:b = 2$. Similarly, with mean values $\mu \approx 1.8$ ms corresponding to a non-dimensionalized mean value $\mu f_0 \approx 1.6$, Fig. 7 indicates that also the reduction in mean time lag observed with increasing aspect ratio $a:b$ of the premix nozzle geometry should have helped to stabilize the combustion instability. However, the reductions in cycle increment computed are stronger than the differences in mean μ and standard deviation σ would suggest – again, see Figs. 6 and 7 – particularly so for the geometry with aspect ratio $a:b = 1.5$. For this case, the mean and standard deviations determined from particle tracking hardly differ from the reference case, while gain and cycle increment are significantly reduced. Deviations of the time lag distribution from the Gaussian shape, i.e. the higher moments of the distribution, account for these discrepancies. To emphasize this point, the gain $|F|$ computed with Gaussian distributions is also shown in the gain plot of Fig. 8. The results for the circular geometry (left graph in the Figure) show that indeed the frequency response computed with time lag distributions determined through particle tracking can be quite different from the one determined from a Gaussian distribution with identical first and second

statistical moment.

Summary and Conclusions

The impact of premix nozzle shape on combustion stability in a geometry representative of an annular low-emission combustor has been investigated by a combination of analytical and numerical means. The flame shape obtained with elliptical premix nozzle geometries of increasing aspect ratio has been computed using a standard stationary Reynolds-averaged formulation with Reynolds-Stress and TFC models for the turbulent reacting flow. From the velocity distribution and the flame shapes computed, the distributions of the fuel transport time lag have been determined by Lagrangian particle tracking. Using a mathematical formalism popular in system identification, the corresponding fuel transport frequency response $F(\omega)$ has been computed and used to achieve closure for a linear acoustic model of a compact premix flame. Using this model for the flame dynamics in a network model of linear acoustic wave propagation and transmission in annular geometries, the impact of nozzle shape on the thermo-acoustic stability of the premix combustor has been explored.

Corroborating the result of an earlier study,⁶ it has been found that a wider distribution of time lags - a larger standard deviation σ - will in general reduce the cycle increment of an unstable mode and eventually stabilize it. The mean value μ of the time lag distribution has also a very strong influence on combustion stability, but it is not possible to find out whether, say, an increase in the mean time lag will suppress or enhance combustion stability without detailed analysis of the relevant phase relationships.¹⁷ The reason for this more complex behavior is that with increasing μ , the fluctuations of heat release due to fuel inhomogeneities go alternately in phase and out of phase with combustor acoustics, promoting or suppressing combustion instability, respectively.^{2,3,6,16,17}

For the configurations investigated, the elliptical

premix nozzles geometries produce wider time lag distributions with smaller mean values than the circular base configuration and are more robust against combustion instabilities. Comparison with results obtained using presumed time lag distributions of Gaussian shape suggests that the reduction in mean time lag μ in this particular instance also contributed to the suppression of the combustion instability. Of course, the increased width of the distribution promotes combustion stability in any case.

Note that in this study, the effects of the elliptical geometry on the formation and growth of coherent structures⁷ and in turn the effects of coherent structures on combustion instability^{8,12} have not been considered. Indeed, the results obtained in this work suggest that the beneficial effects of non-circular nozzle geometry on combustion stability⁵ are not a consequence of the reduced growth and strength of large scale vortices observed in non-circular jets. Instead, it may well be that the changes in flame shape and fuel time lag distribution are the dominant influences. Further investigations are needed to refute or substantiate these conjectures.

In this paper, we presented a combined numerical / analytical method for computing the fuel transport frequency response of a premix nozzle as the z -transform of the unit impulse response \vec{h} of fuel injection and consumption. This novel method is of course in its application not limited to the scope of the present investigation. For example, other passive control methods, e.g. staggered fuel injection or use of non-identical burners within one combustor, can be investigated with this technique.

Nomenclature

Upper Case Letters

- A Cross-sectional area [m²]
- F Fuel transport frequency response [-]
- L Length [m]
- \dot{Q} Rate of heat release per unit area [W/m²]
- M Mach number [-]
- T Temperature [K]
- Y_F Fuel mass fraction [-]

Lower Case Letters

- a Major axis of ellipse [m]
- b Minor axis of ellipse [m]
- c Speed of sound [m/s]
- c_p Specific heat at constant pressure [J/kg-K]
- c_v Specific heat at constant volume [J/kg-K]
- f_0 Frequency of dominant eigenmode [Hz]
- f Downstream Riemann invariant [m/s]
- g Upstream Riemann invariant [m/s]
- g_{cr} Critical rate of strain [1/s]
- \vec{h} Fuel transport unit impulse response [-]
- h_k Width of bins in time lag histogram [s]
- k_x Axial wave number [1/m]

- k_{\perp} Perpendicular wave number [1/m]
- l Length [m]
- l_F Flame stand-off [m]
- \dot{m}_F Fuel mass flow [kg/s]
- p Pressure [Pa]
- t Time [s]
- u Velocity [m/s]
- x Spatial coordinate [m]

Greek Letters

- α Area ratio A_2/A_3
- γ Ratio of specific heats [-]
- δ Dirac function [-]
- ζ Pressure loss coefficient [-]
- Θ Temperature raise coefficient [-]
- λ Wave length [m]
- μ Mean value of time lag distribution [s]
- ξ Ratio of specific impedances [-]
- ρ Density [kg/m³]
- σ Standard deviation of time lag distribution [s]
- τ Time lag [s]
- ϕ Equivalence ratio [-]
- ω Angular frequency [1/s]

Subscripts and Accents

- ' Fluctuation
- 0 Burner plenum
- 1 Location of fuel injection
- 2 End of mixing tube
- 3 Beginning of combustion chamber
- 4 Upstream of flame
- 5 Downstream of flame
- 6 Choked exit

References

- ¹Keller, J. J., "Thermoacoustic Oscillations in Combustion Chambers of Gas Turbines," *AIAA Journal*, Vol. 33, No. 12, 1995, pp. 2280-2287.
- ²Straub, D. L. and Richards, G. A., "Effect of Fuel Nozzle Configuration on Premix Combustion Dynamics," *Int'l Gas Turbine and Aeroengine Congress & Exposition*, ASME **98-GT-492**, Stockholm, Sweden, 1998.
- ³Lieuwen, T., Torres, H., Johnson, C., and Zinn, B. T., "A Mechanism of Combustion Instability in Lean Premixed Gas Turbine Combustors," *Int'l Gas Turbine and Aeroengine Congress & Exposition*, ASME **99-GT-3**, Indianapolis, IN, 1999.
- ⁴Schuermans, B. B. H., Polifke, W., and Paschereit, C. O., "Modeling Transfer Matrices of Premixed Flames and Comparison with Experimental Result," *Int'l Gas Turbine and Aeroengine Congress & Exposition*, ASME **99-GT-132**, Indianapolis, Indiana, USA, 1999.
- ⁵Berenbrink, P. and Hoffmann, S., "Suppression of Dynamic Combustion Instabilities by Passive and Active Means," *Int'l Gas Turbine and Aeroengine Congress & Exposition*, ASME **2000-GT-0079**, Munich, Germany, 2000.
- ⁶Sattelmayer, T., "Influence Of The Combustor Aerodynamics On Combustion Instabilities From Equivalence Ratio Fluctuations," *Int'l Gas Turbine and Aeroengine Congress & Exposition*, ASME **2000-GT-82**, Munich, Germany, 2000.

⁷Gutmark, E. J., "Flow Control with Noncircular Jets," *Ann. Rev. Fluid Mech.*, No. 31, 1999, pp. 239-273.

⁸Coats, C., "Coherent Structures in Combustion," *Prog. Energy Combust. Sci.*, Vol. 22, 1997, pp. 427-509.

⁹Syred, N. and Beer, J. M., "Combustion in Swirling Flows: A Review," *Combust. and Flame*, No. 23, 1974, pp. 143.

¹⁰Syred, N., Gupta, A. K., and Beer, J. M., "Temperature and Density Gradient Changes Arising with the Precessing Vortex Core and Vortex Breakdown in Swirl Burners," The Combustion Institute, 1974, p. 587.

¹¹Paschereit, C. O., Gutmark, E. J., and Weisenstein, W., "Control of combustion driven oscillations by equivalence ratio modulations," *Int'l Gas Turbine and Aeroengine Congress & Exposition*, ASME **99-GT-118**, Indianapolis, IN, 1999.

¹²Paschereit, C. O., Flohr, P., Polifke, W., and Bockholts, M., "Fluid Dynamic Instabilities in a Swirl Stabilized Burner and their Effect on Heat Release Fluctuations," *Proceedings on Flow Induced Vibrations*, Luzern, Switzerland, 2000.

¹³Polifke, W., Paschereit, C. O., and Sattelmayer, T., "A Universally Applicable Stability Criterion for Complex Thermoacoustic Systems," *18. Deutsch-Niederländischer Flammertag*, VDI Bericht, No. 1313, Delft, NL, 1997, pp. 455-460.

¹⁴Dowling, A. P. and Hubbard, S., "Acoustic Instabilities in Premix Burners," *4th AIAA/CEAS Aeroacoustics Conference*, Toulouse, 1998.

¹⁵Dowling, A. P., "Thermoacoustic Instability," *6th Int. Congress on Sound and Vibration*, Copenhagen, Denmark, 1999, pp. 3277-3292.

¹⁶Polifke, W., Paschereit, C. O., and Döbbeling, K., "Suppression of Combustion Instabilities through Destructive Interference of acoustic and Entropy Waves," *6th. Int. Conf. on Sound and Vibration*, Copenhagen, Denmark., 1999.

¹⁷Polifke, W., Paschereit, C. O., and Döbbeling, K., "Constructive and Destructive Interference of Acoustic and Entropy Waves in a Premixed Combustor with a Choked Exit," accepted for publication in *Int. J. of Acoustics and Vibration*, 2001.

¹⁸Karpov, V. P., Lipatnikov, A. N., and Zimont, V. L., "A model of premixed turbulent combustion and its validation," *Archivum Combustionis*, Vol. 14, No. 3-4, 1994, pp. 125-141.

¹⁹Zimont, V. A., Polifke, W., Bettelini, M., and Weisenstein, W., "An Efficient Computational Model for Premixed Turbulent Combustion at High Reynolds Numbers based on a Turbulent Flame Speed Closure," *J. Eng. for Gas Turbines and Power*, Vol. 120, 1998, pp. 526-532.

²⁰Polifke, W., Flohr, P., and Brandt, M., "Modeling of Inhomogeneously Premixed Combustion with an Extended TFC Model," *Int'l Gas Turbine and Aeroengine Congress & Exposition*, ASME **2000-GT-0135**, Munich, Germany, 2000.

²¹Marble, F. E. and Candel, S. M., "Acoustic disturbance from gas non-uniformities convected through a nozzle," *J. of Sound and Vibration*, Vol. 55, 1977, pp. 225-243.

²²T., S. and Stoica, P., *System Identification*, Prentice Hall, 1989.

²³Ljung, L., *System Identification - Theory For the User*, Prentice Hall, 1999, 2nd Edition.

²⁴Polifke, W., Poncet, A., Paschereit, C. O., and Döbbeling, K., "Determination of (Thermo-)Acoustic Transfer Matrices by Time-Dependent Numerical Simulation," *7th Int. Conference on Numerical Combustion*, York, U.K., York, UK, 1998.

²⁵Polifke, W., Poncet, A., Paschereit, C. O., and Döbbeling, K., "Reconstruction of Acoustic Transfer Matrices by Stationary Computational Fluid Dynamics," accepted for publication in *J. of Sound and Vibration*, 2001.